Düzce University Journal of Science & Technology

Research Article

Catalytic Properties of Hydrothermally Synthesized Flower-like $NiO@Fe_3O_4$

Nurdan KURNAZ YETİM [a,*]

[a] *Department of Chemistry, Faculty of Faculty of Arts and Sciences, Kırklareli University, Kırklareli, TURKEY*
nurdankurnazyetim@klu.edu.tr
** Corresponding author's e-mail address: nurdankurnazyetim@klu.edu.tr*

DOI: 10.29130/dubited.721970

ABSTRACT

In this study, flower-like NiO structures were synthesized by hydrothermal method. Then, Fe_3O_4 was doped on NiO that NiO structures gain magnetic properties. TEM (Transmission Electron Microscopy) and SEM (Scanning Electron Microscopy) were used to assess the morphology of the NiO structures. XRD (X-ray Diffraction) was used to evaluate the crystal structures of the NiO structures. Magnetic properties of the NiO structures were investigated using VSM (Vibrating Sample Magnetometry). Catalysis properties of the produced structures were assessed use of products as catalyst in the reduction of 4-nitrophenol (4-NP) was examined. Especially NiO and Fe_3O_4 were found to exhibit excellent catalytic performance for nitrophenol reduction, while $NiO@Fe_3O_4$ magnetic microflowers were found to exhibit very low catalytic activity.

Keywords: *NiO, Fe_3O_4, Flower-like, 4-Nitrophenol, Hydrothermal synthesis*

Hidrotermal olarak Sentezlenen Çiçek benzeri $NiO@Fe_3O_4$'ün Katalitik Özellikleri

ÖZET

Bu çalışmada, çiçek benzeri NiO hidrotermal yöntemle sentezlendi. Daha sonra NiO üzerine, Fe_3O_4 katkılanarak manyetik özellik kazandırıldı. Elde edilen ürünlerin kristal yapıları XRD (X-ışını kırınımı) metodu ile incelenmiştir. Üretilen yapıların morfolojik özellikleri SEM (Taramalı Elektron Mikroskopisi), ve TEM (Geçirimli Elektron Mikroskobisi) ile karakterize edildi. Ayrıca manyetik ölçümleri için VSM (Manyetik Histeresis Ölçümü) analizi yapıldı. Daha sonra ürünlerin, 4-nitrofenolün (4-NP) indirgenmesinde katalizör olarak kullanımı incelendi. Özellikle NiO ve Fe_3O_4'ün nitrofenolün azaltılması için mükemmel katalitik performans sergilediğini görülürken $NiO@Fe_3O_4$ manyetik mikro yapıdaki çiçeklerin çok düşük katalitik aktivite sergilediğini belirlendi.

Anahtar Kelimeler: *NiO, Fe_3O_4, Çiçek benzeri, 4-Nitrofenol, Hidrotermal sentez*

Received: 17/04/2020, Revised: 06/06/2020, Accepted: 11/06/2020

I. INTRODUCTION

Industrial and agricultural wastewaters contain nitrophenol, which is one the most common organic pollutants. Elimination of nitro groups can be accomplished by reducing them to amines groups. Amin groups are less toxic and biodegradable [1,2]. 4-aminophenol (4-AP) is a powerful intermediate which can be used in the synthesis of drugs. 4-aminophenol is also widely used as a corrosion inhibitor, hair colouring agent and, etc [3,4]. Therefore, conversion of nitrophenol to aminophenol is essential for wastewater management where biodegradation of toxic substance can be achieved. It is stated that the main process for the reduction of the nitro group in general can be achieved by methods such as catalytic / electrochemical reduction of nitrobenzene in the presence of strong acids or hydrogenation of nitrobenzene, which involves molecular rearrangement of the phenylhydroxylamine intermediate in the presence of iron-acid [5-8]. In the presence of sodium borohydride ($NaBH_4$), 4-NP can be reduced to 4-AP in aqueous media [9-12]. However, this reduction reaction mechanism works slowly in the absence of a metal catalyst. For this purpose, various metal nanoparticles have been used as catalysts to reduce nitrophenols to aminophenol.

Pt, Ag, Pd and Au nanoparticles are very effective in catalysts reactions and they are commonly used as nanocatalyst [1,13-17]. Noble nanoparticles attract the attention of researchers since they have outstanding properties such as small size, high electron affinity, quantum confinement effect, good magnetic characteristics, etc. Besides, noble nanoparticles exhibit exceptional catalysis properties. Such properties are surface related properties which can be seen on nanoparticle surface. For example, only the electrons at the surfaces of these nanoparticles are used in catalytic reactions where most of the atoms in the nanoparticles are catalytically inactive during the catalysis reaction [3]. Therefore, enhanced surface - volume ratio results in enhanced catalysis activity. Traditionally, flower-like metal oxide nanomaterials have attracted attention in a variety of fields, including catalysis, electronic and analytical sciences, due to their rough surface with large surface / volume ratios [18-21]. Many researchers are willing to use transition metal oxide nanoparticles instead of noble metal nanoparticles. They consider that transition metal oxide nanoparticles are highly reactive, they can be cheaply synthesized and can be an alternative to noble metal nanoparticles [21-23].

Nanocatalysts are quite small hence, it is difficult to separation the nanoparticles from the reaction pot. At this point, nanocomposites are found to be promising to overcome this issue. Nanocomposites are nanoplatforms [24,25]. Thus, special nanocomposites having magnetic properties can be fabricated. Consequently, such nanocatalysts with magnetic properties can be separated from the reaction pot with a strong magnet. Such a case eliminate the need for physical filtration where catalysts can be lost in the filtration process. Materials with superparamagnetic characteristics are suitable candidate to fabricate such nanoplatforms.

In this study, NiO, Fe_3O_4 and NiO@Fe_3O_4 samples were prepared using the hydrothermal method. Various techniques were used in the sample characterization. In the presence of $NaBH_4$, catalysis performance of metal oxide compounds with flower-like morphology was evaluated. Flower-like NiO and Fe_3O_4 were found to exhibit high catalytic activity.

II. MATERIALS AND METHODS

A. MATERIALS, SPECTRAL DATA MEASUREMENTS, AND SYNTHESIS PROCEDURE

All the chemical reagents used in the experimental process are analytical grade pure. No purification process was applied to the chemicals. NaOH (sodium hydroxide), $Ni(ac)_2.4H_2O$ (nickel acetate tetrahydrate), urea ($CO(NH_2)_2$), $FeSO_4.7H_2O$ iron(II) sulphate heptahydrate) were purchased from Sigma-Aldrich.

XRD patterns were recorded using the RIGAKU miniflex600 X-ray diffractometer has a scan range of $10 < 2\theta < 90$. Also, the surface morphology of the nano structures was assessed using a Field Emission Scanning Electron Microscopy (FESEM). In the confirmation of elemental composition, EDX (Energy Dispersive X-Ray) spectrometer was used. FEI Quanta 400F model device was used in FESEM-EDX investigation. TEM studies were carried out on a JEOL JEM 1220electron microscope. Cryogenic Limited PPMS VSM was used in the magnetic measurements which has the maximum magnetic field of 2±Tesla. Shimadzu UV-2600 Ultraviolet-Visible (UV-Vis) spectrophotometer was used in the catalytic study.

A. 1. Synthesis of Flower-like NiO

0.5 g ($Ni(ac)_2.4H_2O$) and 0.25 g $CO(NH_2)_2$ were dissolved in 30 mL ethanol. Mixture was stirred using magnetic stirrer. The homogeneous mixture was then poured in a teflon-lined stainless steel 50mL autoclave. Mixture was kept in oven for 12h at 190 °C. Teflon autoclave was cooled at room temperature. The product was centrifuged to get the precipitate. The precipitate was washed with ethanol and deionized water. The washed precipitate was dried in the oven for 24h at 60 °C. Green powder was obtained and calcination procedure was applied to the powder in an oven for 1 hour where powder was heated with a ramp rate of 10 °C / minute up to 400 °C. Result product was then cooled to room temperature [26].

A. 2. Synthesis of Magnetic Fe_3O_4 Nanostructure

Hydrothermal method was used in the production of magnetic nanoparticles. To this end, 0.656 g $FeSO_4.7H_2O$ and 3.2 g NaOH were dissolved in 40 mL deionized water. The solution was mixed for 10 minutes until it homogenizes, then 50 mL of teflon autoclave covered with stainless steel was placed and left at 150 °C for 6 hours. The resulting black precipitate was collected by centrifugation at 8000 rpm for 20 minutes. The product was washed several times with deionized water and absolute ethanol. Powder like precipitate was treated in vacuum oven at 40 °C for 12 hours [27].

A. 3. Synthesis of Magnetic $NiO@Fe_3O_4$ Nanoflowers

0.1 g $Ni(ac)_2.4H_2O$ was dissolved in 10 mL deionized water using ultrasonic bath. In a separate beaker, 0.13 g $FeSO_4.7H_2O$ was dispersed in 10 mL deionized water. 0.64 g NaOH was added and mixed for 10 minutes. The prepared solution was then poured onto $Ni(ac)_2.4H_2O$. The ultrasonic bath was mixed for a further 5 minutes, a stainless steel coated 40 mL capacity teflon autoclave was taken and kept at 150 ° C for 6 hours. The resulting black precipitate was collected by centrifugation at 8000 rpm for 20 minutes. The product was washed several times with deionized water and absolute ethanol. Powder like precipitate was treated in a vacuum oven at 40 ° C for 12 hours.

A. 4. Catalytic Test

In a typical test, freshly prepared $NaBH_4$ solution (0.2 M, 0.3 mL) was added to 3 mL of 0.1 mM aqueous 4-NP solution. It was scanned on the UV spectrometer between 250nm - 550 nm wavelength. 3 mg of catalyst (NiO, Fe_3O_4 and $NiO@Fe_3O_4$) were added to the mixture and stirred for 1 min at room temperature (25 °C). Reduction of 4-NP to 4-AP was tracked using UV-Vis spectrophotometer.

III. RESULTS AND DISCUSSION

A. CHARACTERIZATION OF NiO, Fe_3O_4 AND NiO@Fe_3O_4

In Figure 1, XRD pattern of flower-like NiO, Fe_3O_4 NiO@Fe_3O_4 structures were presented. In the XRD pattern of NiO, three strong peaks with high density were seen which illustrates (111), (2 0 0) and (2 2 0) crystal orientation. Peaks indicate that prepared NiO is cubic crystal structure [28]. When XRD patterns are examined, sharp peaks prove the pure and well crystallized NiO products that are obtained by hydrothermal synthesis method. When the XRD pattern of Fe_3O_4 magnetic nanoparticles was examined, it was seen that the characteristic peak positions found for the spinel structures in the Fe_3O_4 structures. It has been found that Fe_3O_4 samples are pure, in other words, they are not contaminated, and they do not contain trace of other elements [27,29]. NiO@Fe_3O_4 magnetic nanoflowers were obtained by NiO with Fe_3O_4. XRD pattern of NiO@Fe_3O_4 magnetic nanoflowers revealed that the diffraction peaks that both nano structures have remained. Both peaks observed at the pattern of NiO and peaks observed at the XRD pattern of Fe_3O_4 were seen at the XRD pattern of NiO @Fe_3O_4. Such a case is an indication that both NiO and Fe_3O_4 structures protect their structures which indicate that NiO@Fe_3O_4 structure is in composite form.

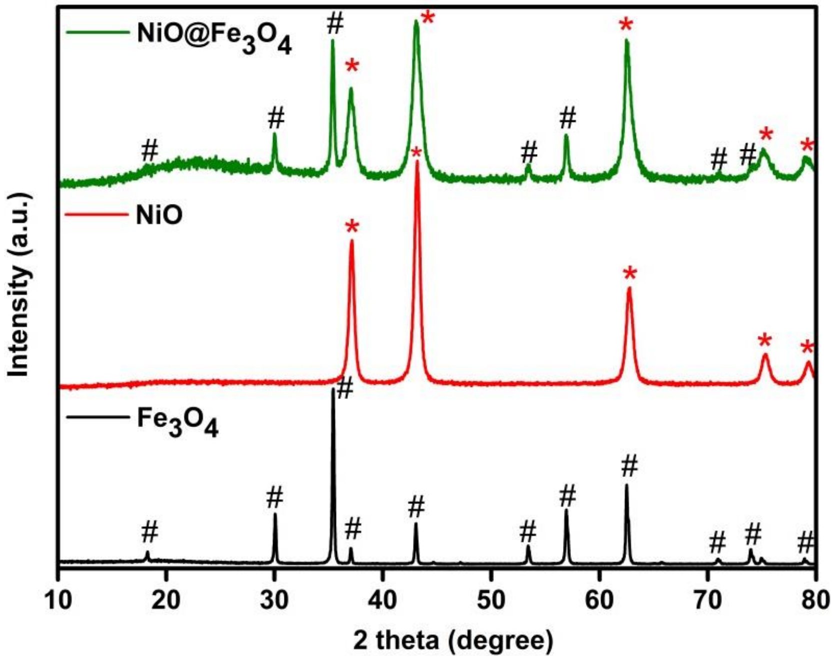

Figure 1. *XRD patterns of NiO, Fe_3O_4 and NiO@Fe_3O_4*

The morphology and microstructure of the samples were analysed by field emission scanning electron microscopy (FESEM). Figure 2 shows low and high magnification FESEM images of flower-like NiO, Fe_3O_4 and NiO@Fe_3O_4 structures. NiO's nano-bowls and nano leaves (nanosheets) were found to turn into well-packed and self-organizing rose-like flowers. Figure 2(e) shows that the Fe_3O_4 magnetic nanoparticles have relatively uniform octahedral morphology. The average diameter of the flower-like NiO was found to be approximately 2.5-3 µm. In addition, FESEM images of NiO@Fe_3O_4 was also obtained. Images confirm that the flower-like structure was preserved. Figure 2(i) shows the high resolution TEM micrograph of single nanosheet of NiO@Fe_3O_4. TEM results are quite consistent with FESEM observations.

Figure 3(c) shows the EDX spectrum of the prepared samples. The presence of Fe atoms in the EDX spectrum of NiO@Fe_3O_4 is a proof that Fe_3O_4 is bound to the NiO microparticle.

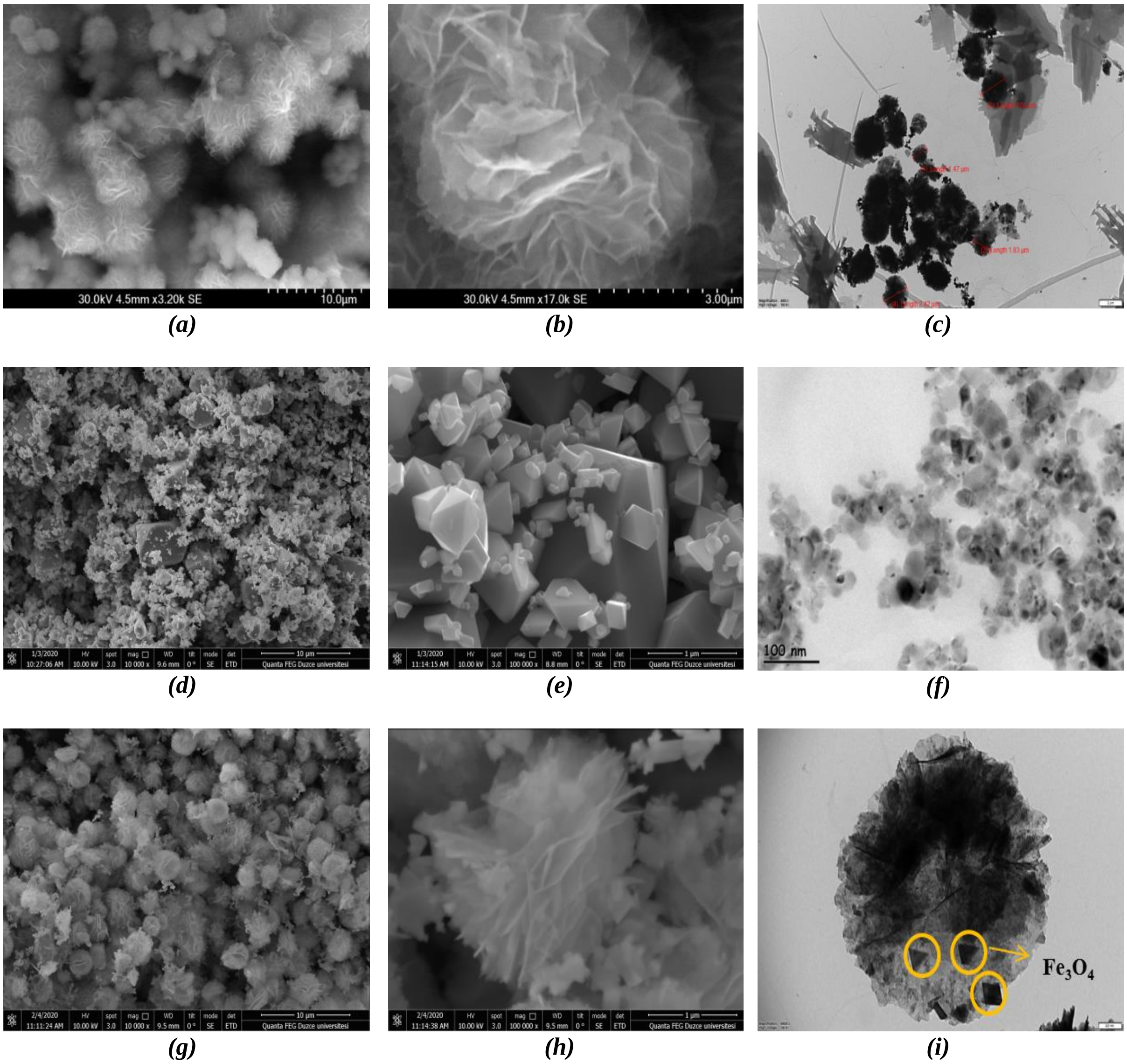

Figure 2. *Low and high magnification FESEM images of as-synthesized NiO* ***(a,b)****, Fe$_3$O$_4$* ***(d, e)****, NiO@ Fe$_3$O$_4$* ***(g,h)*** *and TEM images of the flower-like NiO* ***(c)****, Fe$_3$O$_4$* ***(f)****, NiO@ Fe$_3$O$_4$* ***(i)***

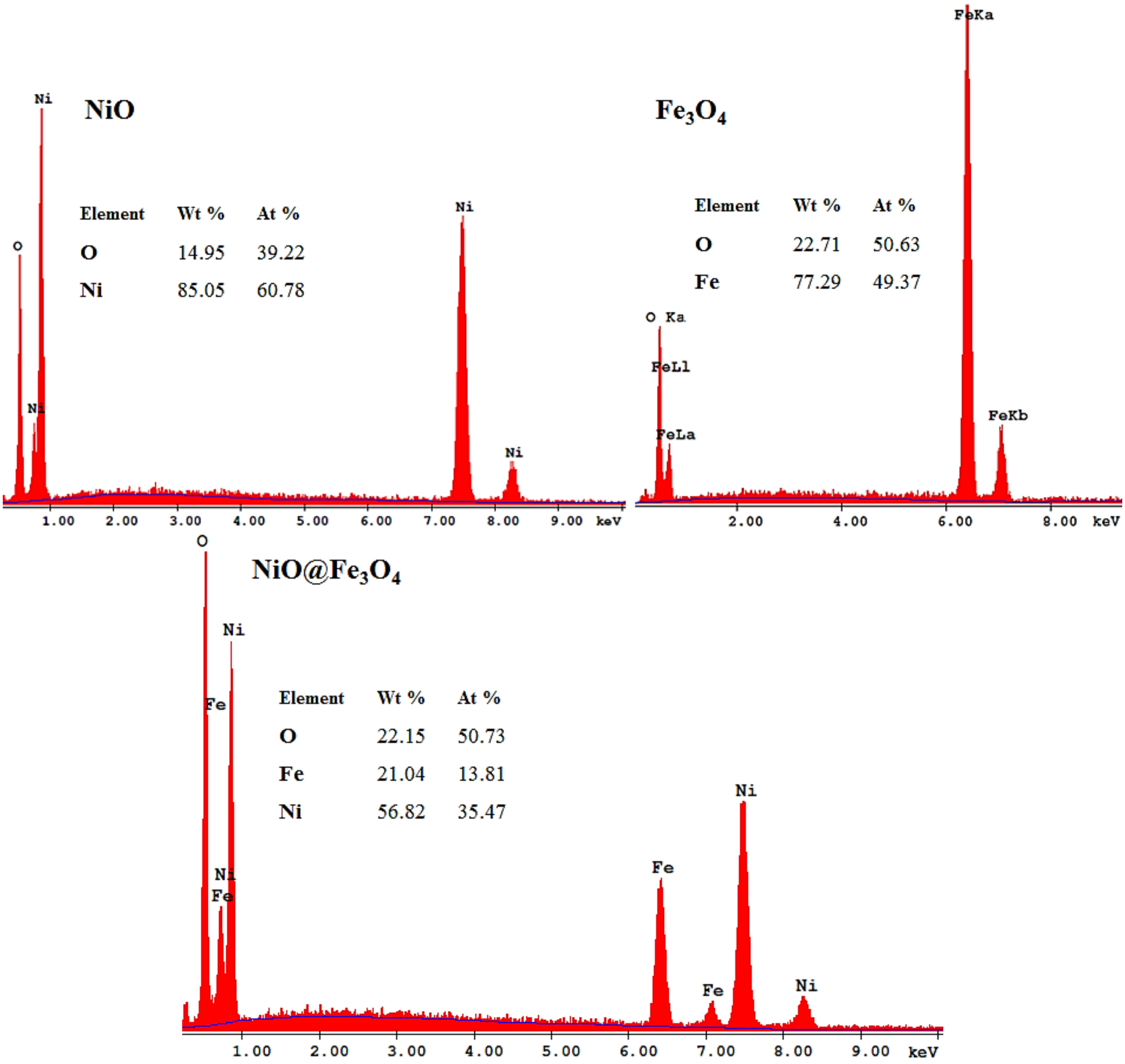

NiO

Element	Wt %	At %
O	14.95	39.22
Ni	85.05	60.78

Fe_3O_4

Element	Wt %	At %
O	22.71	50.63
Fe	77.29	49.37

$NiO@Fe_3O_4$

Element	Wt %	At %
O	22.15	50.73
Fe	21.04	13.81
Ni	56.82	35.47

Figure 3. *EDX spectrum of NiO, Fe_3O_4, $NiO@Fe_3O_4$*

Figure 4 shows the magnetization curves of the Fe_3O_4 and $NiO@Fe_3O_4$ nanoparticles. It was determined that the Fe_3O_4 magnetic nanoparticles obtained after six hours had a superparamagnetic character at room temperature. At this temperature, the saturated magnetization values for the Fe_3O_4 nanoparticle were determined to be 89.8 emu / g. Due to the high crystalline properties of Fe_3O_4 nanoparticles, saturated magnetization value was found to be quite high. Sahin et al. reported the saturated magnetization value for Fe_3O_4 nanoparticles as 52.2 emu g $^{-1}$[30]. Saturated magnetization values of $NiO@Fe_3O_4$ o found as 21.5 emu / g. They also show super paramagnetic characteristics. Mahmoud et al synthesized $Fe_3O_4@NiO$ core-shell nanocomposite by precipitation method to investigate Cr (VI) adsorption efficiency. The saturated magnetization value of the synthesized nanocomposites was found to be 11.5 emu / g for their samples [31]. It is understood that our samples have higher magnetic saturation values than that of results reported in the literature.

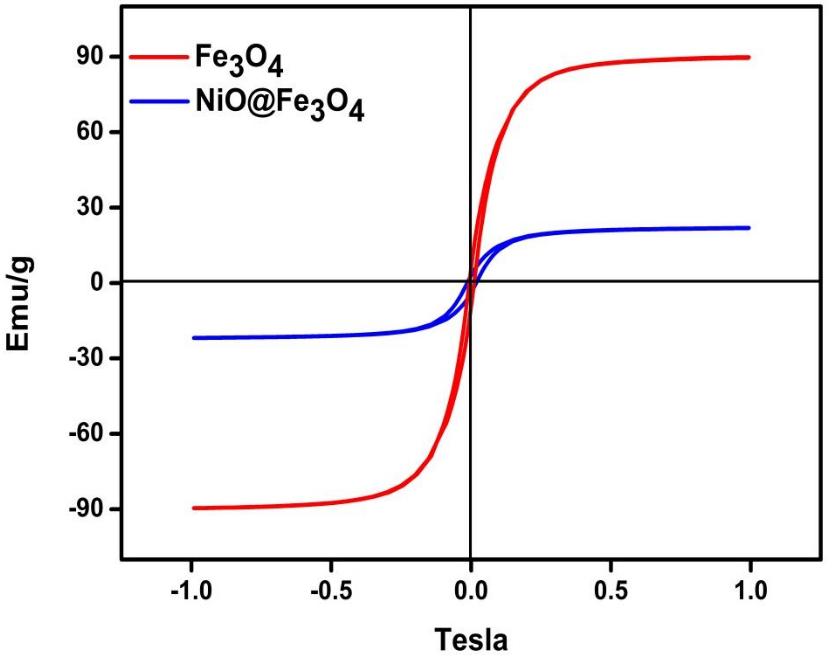

Figure 4. *Magnetic hysteresis of* Fe_3O_4 *and* $NiO@Fe_3O_4$ *nanostructures*

B. CATALYTIC ACTIVITY OF NiO, Fe_3O_4 AND $NiO@Fe_3O_4$

In the presence of $NaBH_4$, the catalytic activities of the samples were investigated for the reduction of nitrophenol to aminophenol. For all experiments, initial concentrations were reacted with 0.1 mM 4-NP and 0.2 M $NaBH_4$, respectively. The bounded peak was seen at UV-Vis spectra at 317 nm which is the indication of 4-NP. After the addition of $NaBH_4$, the peak then shifted to 400 nm region. This peak illustrates the formation of the-p-nitrophenolate ions which was affected from the $NaBH_4$ [32, 33]. Addition of 3 mg of NiO, Fe_3O_4 and $NiO@Fe_3O_4$ nanoparticles result in the simultaneous growth of new peaks which were appeared around 295-300 nm. Such appearance confirms the existence of 4-AP which results in a sudden diminish in the intensity of the peak at 400 nm (See Fig. 5).

When 3 mg of NiO catalyst was added to the medium, the reduction process was observed to occur in 55 minutes, while it was found that this time was reduced when using Fe_3O_4 (38 minutes). Mandlimath and Gopal were found to be completed in about 4 hours in the presence of 0.8 mg commercial NiO catalyst [20].

The efficiency of the reduction reaction using our catalytic samples was investigated where produced samples were added to the reaction medium. To evaluate the reaction efficiency, linear graphs of ln (At / A_0) against time were obtained. The reaction rate was assessed using the diminish in the intensity of 4-NP peak in the UV-Vis spectrum. Figure 5 (d) shows the relation between the absorption peak density and time where absorption peak density was illustrated in natural logarithm form. The slope of the plot was used to calculate the rate constant of the reduction reaction. The rate constant (k_{app}) of the NiO, Fe_3O_4 and $NiO@Fe_3O_4$ compounds were found to be $1.2x10^{-3}$, $1.4x10^{-3}$, $4x10^{-5}$ s^{-1}, respectively. Jiang et al. synthesized nickel nanoparticles in varying sizes and morphologies that was used in the reduction process. All the nickel samples were compared to commercial RANEY Ni. When using RANEY Ni catalyst, the reaction rate constant (k_{app}) was found to be $0.32x10^{-3}$ s^{-1} and showed lower value to other Ni nanoparticles [34].

In the presence of $NaBH_4$, NiO and Fe_3O_4 exhibited the best catalytic activity for the reduction of 4-NP to 4-AP. The catalytic performance of the $NiO@Fe_3O_4$ was found to be low compared to NiO and Fe_3O_4 nanostructures. It was also seen that $NiO@Fe_3O_4$ managed to reduce 20% of product to 4-AP in 70 min.

***Table 1.** Results obtained for the reduction of 4-NP ([4-NP] = 0.1 mM, [$NaBH_4$]= 0.2 M)*

Catalyst *(3 mg)*	**Time** *(min)*	**K_{app} (s^{-1})**	**Conversion** *(%)*	**R^2**
NiO	55	$1.2x10^{-3}$	97.55	0.9981
Fe_3O_4	38	$1.4x10^{-3}$	98.76	0.9748
NiO@ Fe_3O_4	70 <	$4x10^{-5}$	20.17	0.9824

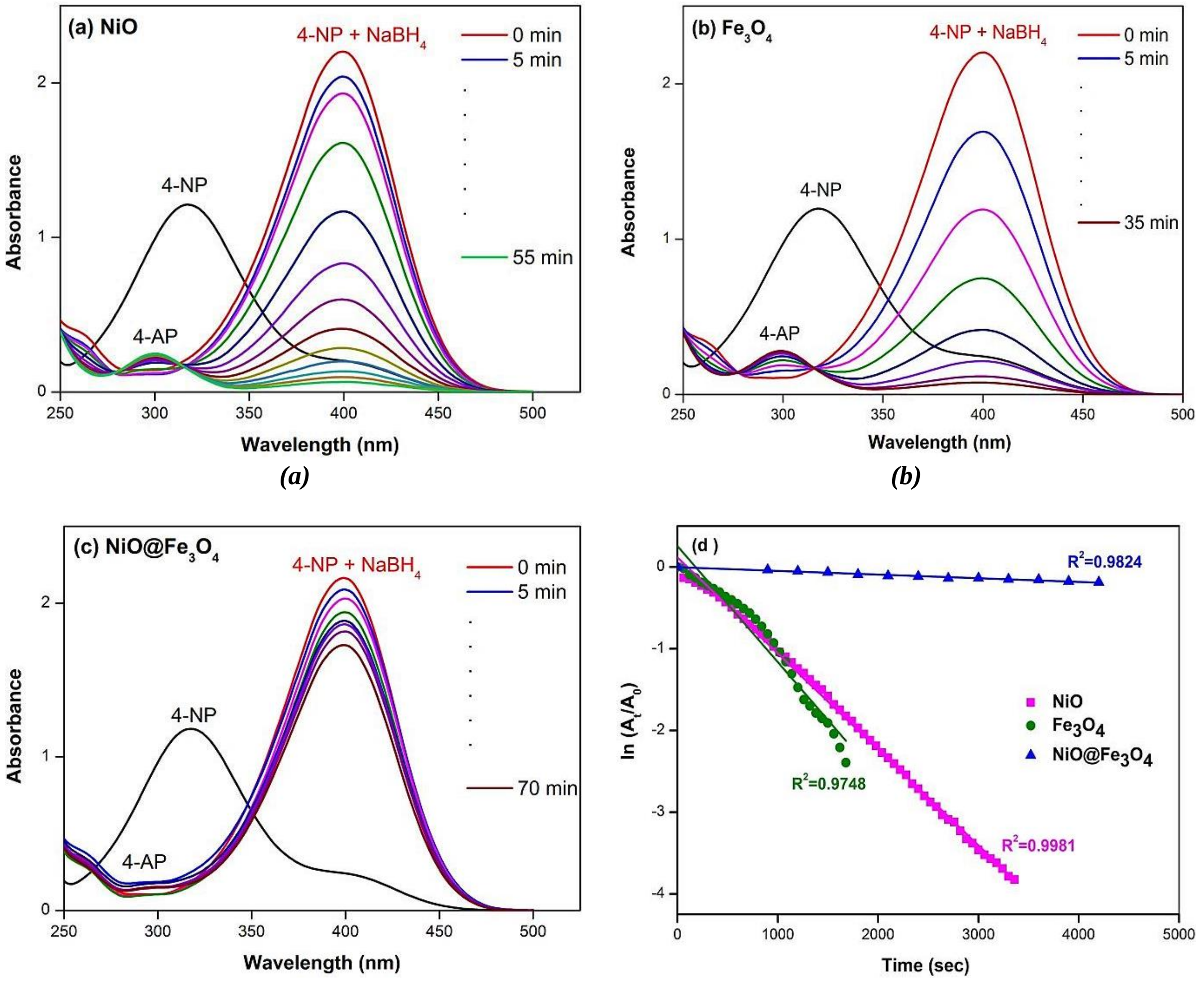

(a) ***(b)***

(c) ***(d)***

***Figure 5.** UV-Vis spectra obtained in the p-nitrophenol reduction in the presence of NiO **(a)**, Fe_3O_4 **(b)** and NiO@Fe_3O_4 **(c)** and rate constants of the reaction **(d)**.*

IV. CONCLUSION

NiO, Fe_3O_4 and NiO@Fe_3O_4 samples were successfully produced using the hydrothermal techniques. The chemical and physical characteristics of the samples were illuminated using various spectroscopic and imaging methods. Flower-like NiO specimens were found to be cubic crystalline, while Fe_3O_4 specimens were in face centred cubic (fcc) crystal form. It was seen that NiO nanoparticles gained magnetic properties with Fe_3O_4 doping. The use of the samples as a catalyst in the reduction process of 4-NP was examined. It is known fact that noble metals are frequently used in this reduction process. It was found that the metal oxide catalysts samples, which were used in this work, showed as high performance as noble metals. The electron transfer mechanism existing on the surface of the noble metals affect the performance of the reduction process. Since our samples has flower like architecture, electron transfer to can be existed in the inner surface samples. As a result, it was illustrated that NiO, Fe_3O_4, NiO@Fe_3O_4 nanostructures showed outstanding catalytical properties. Their catalytic performance is as good as noble metal nanostructures reported in literature.

V. REFERENCES

[1] H. Woo, J. W. Kim, M. Kim, S. Park, K. H. Park, “Au nanoparticles supported on magneticallyseparable Fe_2O_3–graphene oxide hybrid nanosheets for the catalytic reduction of 4-nitrophenol,” *RSC Advances*, vol. 5, no. 10, pp. 7554–7558, 2015.

[2] Y. C. Chang, D. H. Chen, “Catalytic reduction of 4-nitrophenol by magnetically recoverable Au nanocatalyst,” *Journal of Hazardous Materials*, vol. 165, no.1-3, pp. 664-669, 2009.

[3] A. Chinnappan, S. K. Eshkalak, C. Baskar, M. Khatibzadeh, E. Kowsarid, S. Ramakrishna, “Flower-like 3-dimensional hierarchical Co3O4/NiO microspheres for 4-nitrophenol reduction reaction,” *Nanoscale Advances*, vol. 1, pp. 305-313, 2019.

[4] K. Sravanthi, D. Ayodhya, P. Y. Swamy, “Green synthesis, characterization and catalytic activity of 4-nitrophenolreduction and formation of benzimidazoles using bentonite supportedzero valent iron nanoparticles,” *Materials Science for Energy Technologies*, vol. 2, no. 2, pp. 298-307, 2019.

[5] M. J. Vaidya, S. M. Kulkarni, R. V. Chaudhari, “Synthesis of p-aminophenol by catalytic hydrogenation of p-nitrophenol,” *Organic Process Research & Development*, vol. 7, pp. 202-208 2003.

[6] A. H. Abbar, A. H. Sulaymon, M. G. Jalhoom, “Scale-up of a fixed bed electrochemical reactor consisting of parallel screen electrode used for p-aminophenol production,” *Electrochimica Acta*, vol. 53, pp. 1671-1679, 2007.

[7] J. Feng , L. Sua, Y. Ma, C. Ren, Q. Guo, X. Chen, “$CuFe_2O_4$ magnetic nanoparticles: A simple and efficient catalyst for the reduction of nitrophenol,” *Chemical Engineering Journal*, vol. 221, pp. 16-24, 2013.

[8] K. Zhang, J. M. Suh, J.-W. Choi, H. W. Jang, M. Shokouhimehr, R. S. Varma, “Recent Advances in the Nanocatalyst-Assisted NaBH4 Reduction of Nitroaromatics in Water,” *ACS Omega*, vol. 4, no. 1, pp. 483-495, 2019.

[9] A. Mondal, A. Mondal, B. Adhıkary, D. K. Mukherjee, “Cobalt nanoparticles as reusable catalysts for reduction of 4-nitrophenol under mild conditions,” *Bulletin of Materials Science*, vol. 40, no. 2, pp. 321-328, 2017.

[10] A. S. Hashimi, M. A. N. M. Nohan, S. X. Chin, S. Zakaria, C. H. Chia, “Rapid catalytic reduction of 4-Nitrophenol and clock reaction of methylene blue using copper nanowires,” *Nanomaterials*, vol. 9, no. 936, pp. 1-13, 2019.

[11] K. S. Shin, J.-Y. Choi, C. S. Park, H. J. Jang, K. Kim, “Facile synthesis and catalytic application of silver-deposited magnetic nanoparticles,” *Catalysis Letters*, vol. 133, pp. 1-7, 2009.

[12] K. Kalantari, A. B. M. Afifi, S. Bayat, K. Shameli, S. Yousefi, N. Mokhtar, A. Kalantari “Heterogeneous catalysis in 4-nitrophenol degradation and antioxidant activities of silver

nanoparticles embedded in Tapioca starch," *Arabian Journal of Chemistry*, vol. 12, no. 8, pp. 5246-5252, 2019.

[13] S. Pandey, S. B.Mishra, "Catalytic reduction of p-nitrophenol by using platinum nanoparticles stabilised by guar gum," *Carbohydrate Polymers*, vol. 113, pp. 525-531, 2014.

[14] K. Hasan, I. A. Shehadi, N. D. Al-Bab, A. Elgamouz, "Magnetic chitosan-supported silver nanoparticles: A heterogeneous catalyst for the reduction of 4-Nitrophenol," *Catalysts*, vol. 9, no. 839, pp. 1-18, 2019.

[15] V. K. Gupta, N. Atar, M. L. Yolac, Z. Üstündağ, L. Uzun, "A novel magnetic Fe@Au core–shell nanoparticles anchored graphene oxide recyclable nanocatalyst for the reduction of nitrophenol compounds," *Water Research*, vol. 48, no. 1, pp. 210-217, 2014.

[16] L. Ai, J. Jiang, "Catalytic reduction of 4-nitrophenol by silver nanoparticles stabilized on environmentally benign macroscopic biopolymer hydrogel," *Bioresource Technology*, vol. 132, pp. 374-377, 2013.

[17] M. S. Chavali, M. P. Nikolova, "Metal oxide nanoparticles and their applications in nanotechnology," *SN Applied Sciences*, vol. 1, no. 607, pp. 1-30, 2019.

[18] J. Jeevanandam, A. Barhoum, Y. S. Chan, A. Dufresne, M. K. Danquah, "Review on nanoparticles and nanostructured materials: History, sources, toxicity and regulations," *Beilstein Journal of Nanotechnology*, vol. 9, pp. 1050-1074, 2018.

[19] P. Shende, P. Kasture, R.S. Gaud, "Nanoflowers: The future trend of nanotechnology for multi-applications," *Artificial Cells, Nanomedicine, and Biotechnology*, vol. 46, no. S1, pp. 413-422, 2018.

[20] T. R. Mandlimath, B. Gopal, "Catalytic activity of first row transition metal oxides in the conversion of p-nitrophenol to p-aminophenol," *Journal of Molecular Catalysis A: Chemical*, vol. 350, no. 1-2, pp. 9-15, 2011.

[21] B. M. Mogudi, P. Ncube, R. Meijboom, "Catalytic activity of mesoporous cobalt oxides with controlledporosity and crystallite sizes: Evaluation using the reduction of4-nitrophenol," *Applied Catalysis B: Environmental*, vol. 198, pp. 74-82, 2016.

[22] Y. Ma, Y. Ni, F. Guo, N. Xiang, "Flowerlike copper(II)-based coordination polymers particles: Rapid room-temperature fabrication, influencing factors, and transformation toward CuO microstructures with good catalytic activity for the reduction of 4-Nitrophenol," *Crystal Growth & Design*, vol. 15, no. 5, pp. 2243-2252, 2015.

[23] A. H. Kianfar, M. A. Arayesh, "Synthesis, characterization and investigation of photocatalytic and catalytic applications of $Fe_3O_4/TiO_2/CuO$ nanoparticles for degradation of MB and reduction of nitrophenols," *Journal of Environmental Chemical Engineering*, vol. 8, no. 1, pp. 103640, 2020.

[24] Y. Zhong, Y. Gua, L.Yua, G. Cheng, X. Yang, M. Sun, B. He, "APTES-functionalized Fe_3O_4 microspheres supported Cu atom-clusters with superior catalytic activity towards 4-nitrophenol reduction," *Colloids and Surfaces A*, vol. 547 pp. 28-36. 2018.

[25] U. Kurtan, A. Baykal, "Fabrication and characterization of Fe_3O_4@APTES@PAMAM-Ag highly active and recyclable magnetic nanocatalyst: Catalytic reduction of 4-nitrophenol," *Materials Research Bulletin*, vol. 60, pp. 79-87, 2014.

[26] Y. B. Mollamahale, Z. Liu, Y. Zhen, Z. Q. Tian, D. Hosseini, L. Chen, P. K. Shen, “Simple fabrication of porous NiO nanoflowers: Growth mechanism, shape evolution and their application into Li-ion batteries,” *International Journal of Hydrogen Energy,* vol. 42, no. 10, pp. 7202-72110, 2017.

[27] W. Lei, Y. Liu, X. Si, J. Xu, W. Du, J. Yang, T. Zhou, J. Lin, “Synthesis and magnetic properties of octahedral Fe_3O_4 via a one-pot hydrothermal route,” *Physics Letters, Section A: General, Atomic and Solid State Physics*, vol. 381, no. 4, pp. 314-318, 2017.

[28] V. Sudha, S. Murugesan, S. Kumar, R. Thangamuthu, “Synthesis and characterization of NiO nanoplatelet and its application in electrochemical sensing of sulphite,” *Journal of Alloys and Compounds,* vol. 744, pp. 621-628, 2018.

[29] R.Y. Hong, S.Z. Zhang, G.Q. Di, H.Z. Li, Y. Zheng, J. Ding, D.G. Wei, “Preparation, characterization and application of Fe_3O_4/ZnO core/shell magnetic nanoparticles,” *Materials Research Bulletin*, vol. 43, no. 8-9, pp. 2457-2468, 2008.

[30] F. Sahin, E. Turan, H. Tumturk, G. Demirel, “Core–shell magnetic nanoparticles: A comparative study based on silica and polydopamine coating for magnetic bio-separation platforms,” *Analyst*, vol. 137, pp. 5654-5658, 2012.

[31] E. Mahmoudi, M. A. Behnajady, “Synthesis of Fe_3O_4@NiO core-shell nanocomposite by the precipitation method and investigation of Cr(VI) adsorption efficiency,” *Colloids and Surfaces A,* vol. 538, pp. 287-296, 2018.

[32] A. Rostami-Vartooni, M. Nasrollahzadeh, M. Alizadeh, “Green synthesis of perlite supported silver nanoparticles using Hamamelis virginiana leaf extract and investigation of its catalytic activity for the reduction of 4-nitrophenol and Congo red,” *Journal of Alloys and Compounds,* vol. 680, pp. 309-314, 2016.

[33] J. Fu, S. Wang, J. Zhu, K. Wang, M. Gao, X. Wang, Q. Xu, “Au-Ag bimetallic nanoparticles decorated multi-amino cyclophosphazene hybrid microspheres as enhanced activity catalysts for the reduction of 4-nitrophenol,” *Materials Chemistry and Physics*, vol. 207, pp. 315-324, 2018.

[34] Z. Jiang, J. Xie, D. Jiang, X. Wei, M. Chen, “Modifiers-assisted formation of nickel nanoparticles and their catalytic application to p-nitrophenol reduction,” *CrystEngComm*, vol. 15, pp. 560-569, 2013.